Article

Cell PRESS

Dynamics of Fast and Slow Inhibition from Cerebellar Golgi Cells Allow Flexible Control of Synaptic Integration

John J. Crowley,[1] Diasynou Fioravante,[1] and Wade G. Regehr[1,*]
[1]Department of Neurobiology, Harvard Medical School, 220 Longwood Avenue, Boston, MA 02115, USA
*Correspondence: wade_regehr@hms.harvard.edu
DOI 10.1016/j.neuron.2009.09.004

SUMMARY

Throughout the brain, multiple interneuron types influence distinct aspects of synaptic processing. Interneuron diversity can thereby promote differential firing from neurons receiving common excitation. In contrast, Golgi cells are the sole interneurons regulating granule cell spiking evoked by mossy fibers, thereby gating inputs to the cerebellar cortex. Here, we examine how this single interneuron class modifies activity in its targets. We find that $GABA_A$-mediated transmission at unitary Golgi cell $\rightarrow$ granule cell synapses consists of varying contributions of fast synaptic currents and sustained inhibition. Fast IPSCs depress and slow IPSCs gradually build during high-frequency Golgi cell activity. Consequently, fast and slow inhibition differentially influence granule cell spike timing during persistent mossy fiber input. Furthermore, slow inhibition reduces the gain of the mossy fiber $\rightarrow$ granule cell input-output curve, while fast inhibition increases the threshold. Thus, a lack of interneuron diversity need not prevent flexible inhibitory control of synaptic processing.

INTRODUCTION

When neurons receive a common excitatory input, inhibition can provide dynamic and differential control over their spike output. This can entail modifying the relationship between input excitation and output firing rates (Chance et al., 2002; Mitchell and Silver, 2003; Vogels and Abbott, 2009) or varying the timing of spikes from the neuron (Cobb et al., 1995; Pouille and Scanziani, 2001, 2004; Somogyi and Klausberger, 2005; Wehr and Zador, 2003). Typically multiple types of interneurons provide inhibition with distinct properties to selectively control different aspects of neuronal spike output (Banks et al., 2000; Freund and Buzsaki, 1996; Glickfeld and Scanziani, 2006; Gupta et al., 2000; Hefft and Jonas, 2005; Klausberger et al., 2003; Markram et al., 2004; McBain and Fisahn, 2001; Miles et al., 1996; Pouille and Scanziani, 2004; Tamas et al., 2003). In the cerebellar cortex individual mossy fibers excite many granule cells, yet granule cells are inhibited only by a single class of interneuron, Golgi cells

(Eccles et al., 1967; Palay and Chan-Palay, 1974). While Golgi cells are known to play an important role in motor control (Watanabe et al., 1998), the extent to which they can promote differential firing in granule cells and regulate specific aspects of granule cell firing remains an open question.

Previous studies suggest that populations of Golgi cells can provide multiple types of inhibition. Golgi cell synapses onto granule cells are made within a glomerulus consisting of a mossy fiber bouton, 50 to 100 granule cell dendrites, and Golgi cell axons that have tens to hundreds of release sites (Hamori and Somogyi, 1983; Jakab and Hamori, 1988). Direct synaptic contacts between Golgi cells and granule cells produce fast IPSCs mediated primarily by $\alpha 1$-containing $GABA_A$ receptors (Nusser et al., 1998; Rossi and Hamann, 1998; Farrant and Brickley, 2003). In addition, the close spacing of release sites and scarcity of intervening glia within the glomerulus allow neurotransmitter to diffuse and act at distal sites beyond the opposing postsynaptic density (DiGregorio et al., 2002; Mitchell and Silver, 2000a, 2000b; Nielsen et al., 2004; Rossi and Hamann, 1998; Xu-Friedman and Regehr, 2003). This spillover transmission creates slow indirect IPSCs (Rossi and Hamann, 1998), as well as heterosynaptic modulation of mossy fiber and Golgi cell inputs (Mitchell and Silver, 2000a, 2000b). Furthermore, high affinity $\alpha 6$-containing $GABA_A$ receptors render granule cells sensitive to ambient GABA levels in the glomerulus, creating a tonic conductance that dampens excitability (Brickley et al., 1996; Hamann et al., 2002; Kaneda et al., 1995; Wall and Usowicz, 1997). Ultrastructural studies show that within a glomerulus the number and size of connections made by Golgi cell axons to granule cells is highly variable and 40% of granule cells are not directly contacted by a Golgi cell axon (Jakab and Hamori, 1988). These observations suggest that the potential for variation in the time course and properties of inhibition may be present at individual Golgi cell $\rightarrow$ granule cell synapses.

Our understanding of the functional role of Golgi cell inhibition has been limited by the fact that the properties of individual Golgi cell $\rightarrow$ granule cell connections have not been characterized in detail. Moreover, the properties of this synapse during elevated Golgi cell firing at rates observed in vivo (Holtzman et al., 2006; van Kan et al., 1993; Vos et al., 1999) has not been studied. As a consequence, studies of the effects of inhibition on the input-output relationship at the mossy fiber to granule cell synapses have focused on steady-state conditions and regulation by tonic inhibition provided by the Golgi cell (Mitchell and Silver, 2003; Rothman et al., 2009).
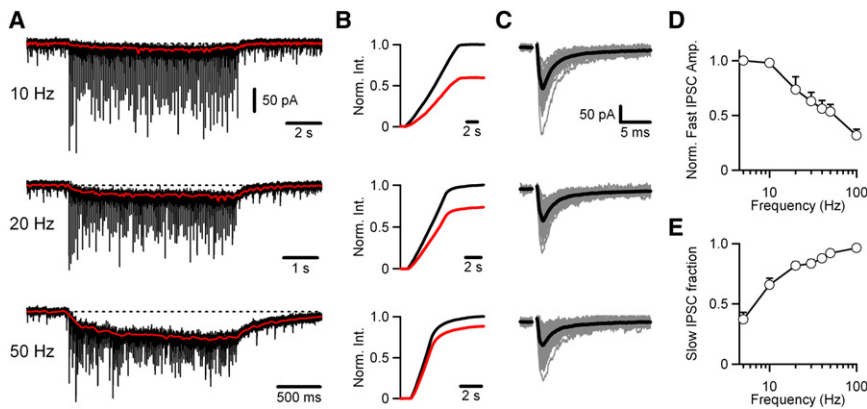
Figure 1. Frequency Dependence of Fast and Slow IPSCs at the Golgi Cell → Granule Cell Synapse

(A) Representative traces of IPSCs recorded in a granule cell in response to trains of extracellular stimulation at 10, 20, and 50 Hz. Each train is the average of three trials of 100 stimuli at each frequency. The superimposed red traces depict the slow component of the IPSC (see Figure S1), and the dotted line denotes the baseline current.

(B) Normalized integrals of the total IPSC (black lines) and the slow IPSC (red lines) during the trains shown in (A).

(C) Individual fast IPSCs (gray traces) are shown superimposed and baseline subtracted, along with the average event (black trace) for each train shown in (A).

(D) Normalized fast IPSC amplitude versus frequency (n = 4 cells).

(E) Average fraction of IPSC charge carried by the slow IPSC versus frequency (n = 4 cells).

Here, we investigate the properties of individual Golgi cell → granule cell synapses during elevated Golgi cell activity. We find that there is considerable diversity in the properties of individual synapses: some are dominated by fast IPSCs, others consist only of slow IPSCs, and many have both fast and slow components. The slow IPSC dominates charge transfer during high frequency trains and is evident even in the absence of direct synaptic contacts. Dynamic clamp studies of the effect of Golgi cell inhibition on granule cell firing suggest that the two types of inhibition have differential effects on the timing and number of spikes evoked by mossy fiber input. Fast IPSCs are most effective at suppressing granule cell firing early in the stimulus train, whereas the slow IPSC dramatically reduces late spikes during sustained mossy fiber activity. Fast and slow inhibition also differentially regulate the input-output curves at the mossy fiber → granule cell synapse, with the slow component selectively reducing the gain and the fast component affecting the threshold of activation. Together these findings suggest that a single type of interneuron can regulate activity in different ways with distinct functional consequences.

RESULTS

The Frequency Dependence of Golgi Cell → Granule Cell Synapses

We examined the frequency dependence of inhibition at the Golgi cell → granule cell synapse by stimulating Golgi cell axons with an extracellular electrode placed in the granular layer and recording IPSCs in granule cells. Synapses were activated with 100 stimuli at 5 to 100 Hz, with excitatory transmission blocked. Low-frequency spontaneous IPSCs were observed in the absence of stimulation. Stimulation evoked inhibitory currents that consisted of fast IPSCs (Figure 1A) riding atop a slow IPSC component (Figure 1A, red traces; see Figure S1 available online). Increases in stimulus frequency increased the amplitude of the slow IPSC, whereas the amplitude of the fast IPSCs decreased. The relative contribution of the fast and slow components of the IPSC was determined by integrating the

currents measured in Figure 1A to quantify the total synaptic charge (Figure 1B, black) and then by integrating the slow component of the synaptic current (Figure 1B, red), with the traces normalized to the total IPSC integral. For the examples shown, the slow IPSC carried 59% and 88% of the total synaptic charge at 10 Hz and 50 Hz, respectively. In the representative experiment, the fast IPSCs decreased from 130 pA at 10 Hz to 75 pA at 50 Hz (Figure 1C). Average fast IPSC amplitudes decreased steadily above stimulation frequencies of 10 Hz, reaching 32% ± 6% of their initial value at 100 Hz (Figure 1D, n = 4 cells). The fractional contribution of the slow component increased from 37% ± 6% at 5 Hz to 96% ± 2% at 100 Hz (Figure 1E, n = 4 cells). These data suggest that for these experimental conditions fast IPSCs are most prominent at low-stimulus frequencies, but the slow IPSC dominates at higher frequencies.

Previous studies have shown that granule cells express high affinity α_6-containing GABA$_A$ receptors, which can be enriched extrasynaptically (Nusser et al., 1998) and may preferentially carry the slow IPSC (Hamann et al., 2002; Rossi and Hamann, 1998). We determined the dependence of the slow IPSC on these receptors by evoking trains in the presence of furosemide. Although this drug can block KCl cotransporters (Payne, 1997), it only blocks those GABA$_A$ receptors containing the α_6 subunit (Korpi et al., 1995). Furosemide (100 μM) decreased the amplitude of the total IPSC integral by approximately 50% but did not selectively reduce the fraction carried by the slow IPSC (Figure S2). The inhibitory currents were eliminated by bicuculline (20 μM; data not shown). Overall, these data suggest that under these conditions both α_1 and α_6-containing GABA$_A$ receptors contribute to the fast and slow components of the Golgi cell → granule cell IPSC.

Properties of Individual Golgi Cell → Granule Cell Connections

Electron microscopic reconstructions indicate that dendrites from many granule cells are contained within a single glomerulus, but Golgi cell axons make direct contacts onto only 60% of them (Jakab and Hamori, 1988). If direct synapses mediate
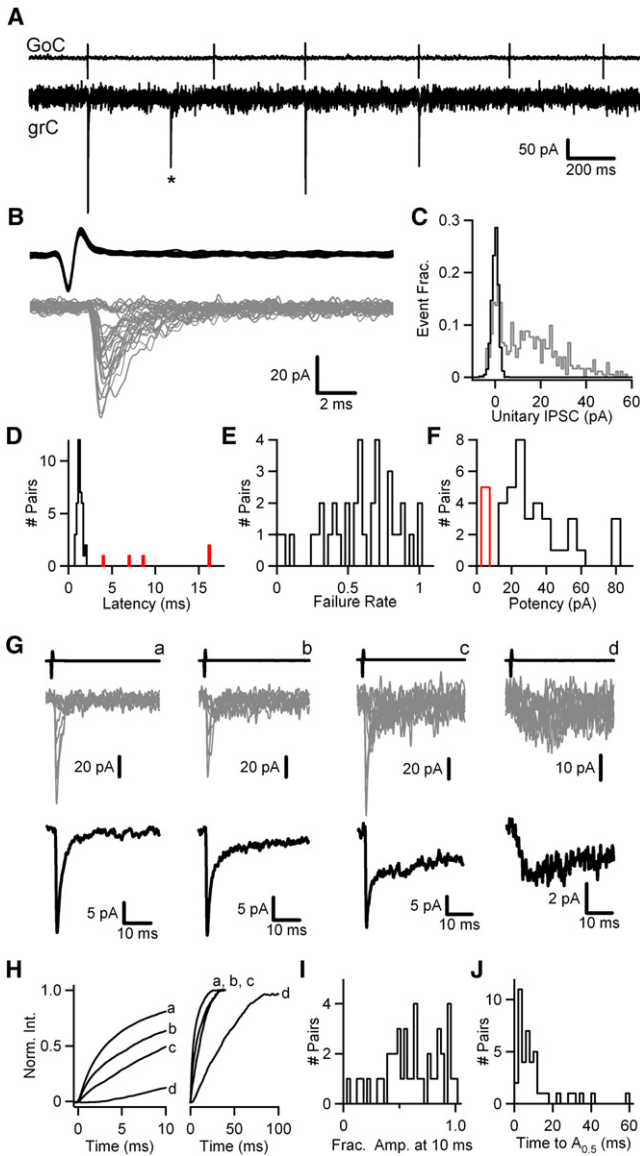
Figure 2. Diversity in the Contribution of Fast and Slow IPSCs at Individual Golgi Cell → Granule Cell Connections

(A) Representative recording of spontaneous activity at a Golgi cell → granule cell connection, showing spikes in the presynaptic Golgi cell (upper) and the corresponding responses in the granule cell (lower). The asterisk denotes an event not temporally linked to spiking in the Golgi cell being monitored.

(B) Twenty-five superimposed Golgi cell spikes (upper), and corresponding granule cell IPSCs (lower, gray traces) from the experiment shown in (A).

(C) Normalized amplitude histogram of 500 events from the same experiment (gray), along with an amplitude histogram of the baseline preceding the event (black).

(D) Histogram of the IPSC latency, defined as time between the peak of the downward deflection of the presynaptic spike and the peak of the first derivative of the average unitary IPSC. Pairs lacking a fast IPSC are shown in red. Histogram of failure rate (E) and potency (F) for 36 Golgi cell → granule cell connections. The average unitary IPSC amplitude for 5 additional pairs lacking a fast IPSC are shown in red.

(G) Sample traces from four individual Golgi cell → granule cell connections (a–d) depicting the average presynaptic spike (upper), 10 superimposed IPSCs

fast IPSCs and nearby release sites onto other granule cells mediate slow IPSCs via spillover as suggested by previous work (Rossi and Hamann, 1998), these morphological studies suggest that there is likely to be diversity with regard to the contribution of fast and slow IPSCs at individual synapses. Moreover, for granule cells receiving direct Golgi cell synapses the size and number of these connections is variable (Jakab and Hamori, 1988), suggesting the efficacy of the fast IPSC is not uniform across individual synapses. We tested these possibilities by examining inhibition at individual Golgi cell → granule cell connections.

Paired recordings were made with a whole-cell electrode to record postsynaptic responses in granule cells and an on cell electrode to monitor spontaneous Golgi cell firing. Twenty-six percent (42/163) of the cell pairs studied were connected. In a representative pair (Figures 2A–2C) a fraction of presynaptic Golgi cell spikes are accompanied by a large short-latency synaptic current in the granule cell with a prominent fast IPSC. The latency, measured from the peak of the downward deflection of the spike to the peak of the first derivative of the average unitary IPSC, was 1.3 ms for this pair. In addition to these short-latency IPSCs, there were also IPSCs observed that were not linked to spiking in the Golgi cell being monitored (Figure 2A, *). It is likely that such IPSCs are evoked by spontaneous firing of other Golgi cells. Putative connections were analyzed using Golgi cell spike-triggered averages of the granule cell recording. A subset of 25 Golgi cell spikes are shown for the sample pair (Figure 2B, upper) along with the corresponding postsynaptic currents (Figure 2B, lower, gray traces), which exhibited a broad amplitude distribution (Figure 2C). This pair had an average unitary IPSC amplitude of 14 pA, a failure rate of 0.48, and a potency (average of successes) of 26 pA. At 36 connections exhibiting a fast IPSC, the latencies were similarly short and narrowly distributed, with a mean of 1.15 ± 0.05 ms (Figure 2D, black). The functional properties of these short-latency connections varied considerably. The failure rate (Figure 2E) and potency (Figure 2F) at each pair was broadly distributed with an average potency of 32 ± 3 pA (n = 36, Figure 2F, black) and an average failure rate of 0.58 ± 0.04 (n = 36, Figure 2E). Thus, the efficacy of the fast IPSC varies markedly between pairs. Interestingly, a small subset of pairs (5/42) exhibited unitary IPSCs with markedly longer latencies, averaging 10 ± 2.5 ms (Figure 2D, red) and had very small unitary IPSC amplitudes, averaging 3.0 ± 0.4 pA (Figure 2F, red). As discussed below, these long-latency connections lack a fast component of inhibition. These data highlight the variation in the functional properties of individual Golgi cell → granule cell connections.

To examine the relative contribution of fast and slow IPSCs at a Golgi cell → granule cell pair, the time course of charge

(middle, gray), and the average unitary IPSC (lower, black) from 58 to 253 events at each pair.

(H) Average unitary IPSCs from (G) are shown integrated and normalized to their peak. The integrated currents are plotted over the first 10 ms (left) and 100 ms (right).

(I) Histogram of the fractional amplitude at 10 ms of IPSCs from 42 Golgi cell → granule cell connections.

(J) Histogram of the half-amplitude times for the same IPSCs shown in (I).

transfer following a spike was quantified. A subset of 10 IPSCs from four sample connections (Figure 2G, middle, gray traces) are shown aligned to the presynaptic spike (Figure 2G, upper), along with the average unitary IPSC (Figure 2G, lower, black trace). Connections differed markedly with regard to their time course (Figures 2Ga–2Gd, lower). In some cases pairs exhibited a large fast IPSC that decayed rapidly (Figure 2Ga). In others, which correspond to the long-latency pairs discussed above, an exclusively slow IPSC was observed (Figure 2Gd). In addition, many pairs exhibited fast IPSCs with slower decays indicative of a progressively larger contribution of the slow IPSC at that connection (Figures 2Gb and 2Gc). To quantify this variation in the time course of synaptic currents across Golgi cell → granule cell pairs, the unitary IPSC was integrated and normalized to the peak of the integral. The fractional IPSC charge at ten milliseconds after onset (Figure 2H, left) ranged from 12% for the pair with the exclusively slow IPSC (Figure 2Gd) to 81% for the pair with the rapidly decaying fast IPSC (Figure 2Ga), and from approximately 5% to 100% across all 42 connections (Figure 2I). Over longer time scales (Figures 2H, right, and 2J) the time to half-amplitude ($A_{0.5}$) exhibited a broad distribution, with a peak near 10 ms and a tail consisting of pairs with larger contributions of the slow IPSC. These data indicate that the contribution of fast and slow IPSCs, as reflected in the time course of the unitary IPSC across Golgi cell → granule cell connections, varies markedly.

Inhibition Mediated by Individual Golgi Cell → Granule Cell Synapses during High-Frequency Activation

We next sought to determine the properties of individual synapses during activation with stimulus trains. On-cell recordings allowed us to noninvasively monitor the properties of individual synapses, but they are limited by the reliance on synapses driven by the spontaneous Golgi cell activity. To allow activation of individual Golgi cells in this configuration, we generated a lentivirus to express mCherry-tagged channelrhodopsin-2 (ChR2) in the cerebellum under the control of the synapsin I promoter (Boyden et al., 2005). Brief blue light pulses (1 ms, 473 nm) of increasing intensity delivered to the soma of a ChR2-expressing Golgi cell (Figure 3A) produced progressively larger depolarizations, sufficient to reach the action potential threshold (Figure 3B). Golgi cell firing could be entrained by brief suprathreshold blue light pulses (Figure 3C). The currents evoked by these light pulse trains show desensitization (Figure 3D, upper) but are still able to drive 50 Hz firing of Golgi cells and precisely maintain a single spike per light pulse (Figure 3D, lower).

We compared the properties of inhibition evoked by spontaneous Golgi cell firing or blue light pulses at the soma (Figures 3E–3G). A sample paired recording with a ChR2-expressing Golgi cell is shown in Figure 3E, in which IPSCs are recorded during spontaneous firing and when firing is entrained at the spontaneous frequency with light. Overlaying average spontaneous IPSCs (Figure 3F, left, gray/black traces) and those evoked by ChR2 at the same frequency (Figure 3F, right, light/dark blue traces) demonstrates that release is not obviously perturbed by light activation. A plot of spontaneous IPSC amplitude against ChR2-evoked amplitude falls along the unity line
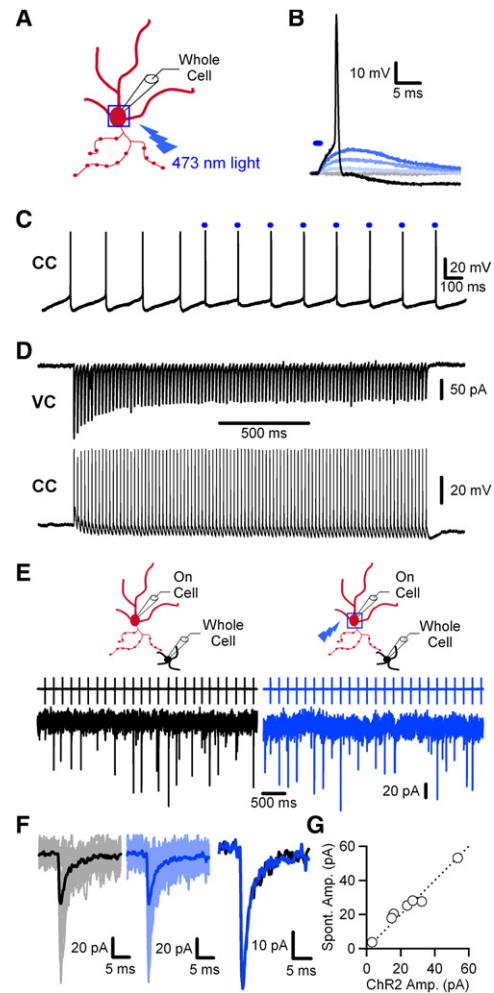

Figure 3. Using Channelrhodopsin-2 to Study Individual Golgi Cell → Granule Cell Synapses

(A) Schematic depicting the typical region, a box around the soma, used for light activation of Golgi cells. A whole-cell electrode was used to monitor membrane potential during light activation of the cell.

(B) Representative recording of ChR2-evoked depolarization of a Golgi cell with brief stimulus (denoted by the blue bar) of increasing intensity (1 ms pulse, 1–2 V applied to 50 mW 473 nm laser).

(C) Sample recording of the entrainment of Golgi cell firing with brief suprathreshold blue light pulses (denoted by the blue bars).

(D) Example recording from a ChR2-expressing Golgi cell of a train of 100 1 ms light pulses delivered at 50 Hz in voltage clamp (upper) and current clamp (lower).

(E) Representative paired recording with a ChR2-expressing Golgi cell. An on-cell electrode was used to monitor Golgi cell spikes and unitary IPSCs were recorded from a granule cell with a whole-cell electrode. IPSCs were recorded either during spontaneous Golgi cell firing (left, black) or when Golgi cells were stimulated with light at approximately the rate of spontaneous firing (right, blue).

(F) Overlay of 25 granule cell IPSCs, along with the average unitary IPSC, from spontaneous activity (left, gray/black traces) or from ChR2-evoked activity (right, light/dark blue traces). The average unitary IPSC from spontaneous firing (far right, black trace) is shown overlayed with the average ChR2-evoked current (far right, blue trace).

(G) Summary plot of the average spontaneous IPSC amplitude plotted against the average ChR2-evoked IPSC amplitude (n = 7 pairs).
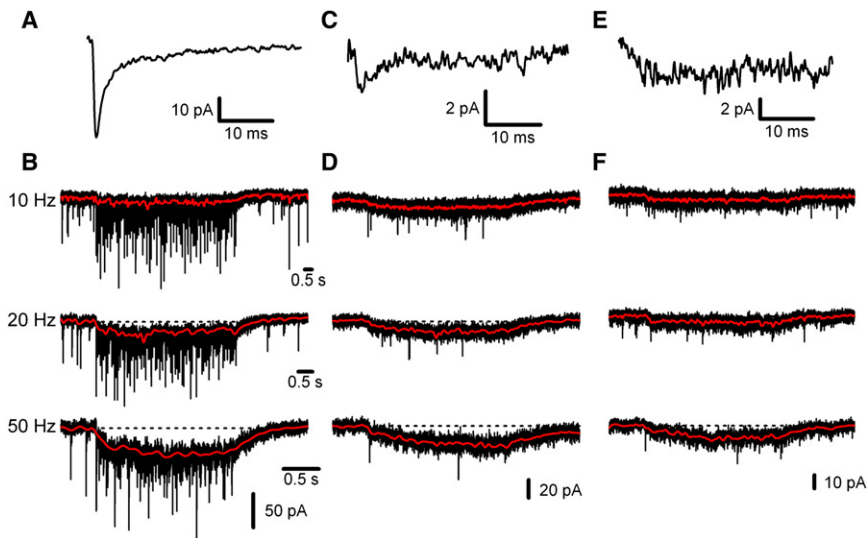
Figure 4. Properties of IPSCs Evoked by Trains of Activity at Diverse Golgi Cell → Granule Cell Pairs

Properties of single Golgi cell → granule cell synapses were examined using spontaneous activity to determine the average IPSC (A, C, and E), as in Figure 2, and using light to evoke spikes in ChR2 expressing cells at 10 Hz, 20 Hz, and 50 Hz (B, D, and F). In the first pair (A and B), a large reliable fast IPSC was observed (A, 82 events), in the second pair (C and D) smaller fast IPSCs occurred only at low rates (C, 100 events), and the third connection (E and F) contained only a small slow IPSC (E, 94 events).

(B, D, and F) The red traces depict the slow component of the IPSC during stimulus trains, and the dotted lines denote the baseline current.

(Figure 3G, n = 7 cells). Overall, these data indicate that ChR2 precisely and reliably drives Golgi cell spiking and does not alter properties of release under our conditions.

We used ChR2 to evoke trains of Golgi cell activity in connected pairs. Figure 4 shows sample trains of 100 stimuli at 10 Hz, 20 Hz, and 50 Hz evoked at three connections with differing properties. The firing of the presynaptic Golgi cell was always monitored with an on-cell electrode, and postsynaptic events were detected using a presynaptic spike-triggered average. In the first sample pair, spontaneous activity in the Golgi cell produced a unitary IPSC with a large, reliable fast component (failure rate = 0.1, potency = 56 pA, unitary amplitude = 51 pA) and an $A_{0.5}$ of 15 ms (Figure 4A). High-frequency activation at this pair evoked large fast IPSCs and, as observed in extracellular stimulation experiments, a slow IPSC that became increasingly prominent with increases in stimulation frequency (Figure 4B, red traces). The slow IPSC contributed 55% of the charge at 10 Hz, increasing to 87% at 50 Hz. In a second pair, Golgi cell stimulation at 10 Hz evoked a unitary IPSC with a smaller, less reliable fast component (potency = 17 pA, failure rate = 0.88, unitary amplitude = 3 pA) and a longer $A_{0.5}$ of 23 ms (Figure 4C). A prominent slow IPSC, that carried 90% to 99% of the charge as the Golgi cell firing rate increased from 10 Hz to 50 Hz, was still evident (Figure 4D). At the third connection, which contained no fast IPSC (average = 4 pA, $A_{0.5}$ = 34 ms; Figure 4E), trains of Golgi cell activity evoked a slow IPSC that carried all of the charge and increased in amplitude with stimulation frequency (Figure 4F). The small phasic events seen in Figure 4F are not linked to the spiking of the activated Golgi cell and likely arise from activity in a different cell. These findings indicate that high-frequency firing in a single Golgi cell is sufficient to produce a prominent slow IPSC during high-frequency trains, even in the absence of a fast IPSC from a direct connection. The slow IPSC grows with increases in the firing rate to dominate charge transfer (range = 78%–100% at 50 Hz, n = 9), similar to our observations with extracellular stimulation.

Differential Functional Roles of Fast and Slow Inhibition

Our data demonstrate that fast IPSCs and slow IPSCs contribute to Golgi cell inhibition of granule cells differentially between individual connections and across Golgi cell firing rates. We wanted to determine the functional consequences of heterogeneity in the time course of inhibition with regard to synaptic integration in granule cells. Specifically, we sought to understand how fast and slow inhibition influence the timing of spikes during a train of mossy fiber input and how they shift the relationship between mossy fiber input and granule cell output across frequencies. To address these issues we used dynamic clamp recordings, which are feasible given that granule cells are electrically compact (Silver et al., 1996). To determine how the time course of inhibition alters the integration of excitatory input by granule cells, we delivered inhibitory waveforms corresponding to 50 Hz Golgi cell firing. Granule cell activity was driven with regular trains of mossy fiber input, including both the AMPA and NMDA component (Figure 5A, black), based on properties of mossy fiber EPSCs recorded in voltage clamp (Figure S3). When delivered to the granule cell, along with tonic inhibition (0.1–0.3 pS), trains of action potentials were generated (Figure 5B, black). Inhibition consisted of either a train of fast IPSCs (Figure 5A, red), a slow IPSC (Figure 5A, blue), or mixed inhibition where the fast IPSC train and slow IPSC contribute equally (Figure 5A, purple). The total inhibitory charge was constant for all three conditions. Fast (Figure 5B, red), slow (Figure 5B, blue), and mixed (Figure 5B, purple) inhibition all reduced the number of spikes generated in response to the excitatory conductance, though spike timing within the train was differentially affected. To quantify this, spike numbers were binned into 100 ms intervals for the duration of the stimulation, normalized to the control frequency in the first bin, and plotted versus time. Relative to control conditions (Figure 5C, black), fast inhibition (Figure 5C, red) decreased the initial spike rate by approximately 60%, while slow inhibition decreased the initial spike rate by less than 20% (Figure 5C, blue). During the last half of the train, the spike rate during fast inhibition remained relatively stable over time and reduced
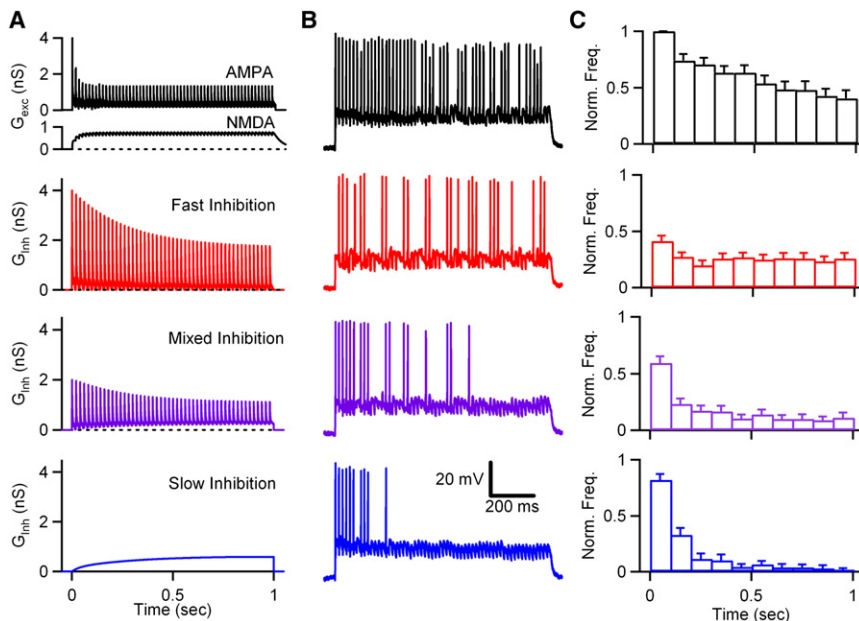
Figure 5. Differential Effects of Fast and Slow Inhibition on the Timing of Spikes Evoked by Trains of Excitation in Granule Cells

Dynamic clamp was used to examine the spiking evoked in granule cells by trains of mossy fiber activity. The properties of AMPA and NMDA conductances were determined by activating mossy fibers and measuring the resulting EPSCs in granule cells (Figure S3). AMPA and NMDA conductances are shown for 60 Hz stimulation in a sample cell (A, black). The conductance waveforms are also shown for inhibition consisting of either fast inhibition alone (A, red), slow inhibition alone (A, blue), or mixed inhibition (A, purple) evoked by a 50 Hz train of Golgi cell activity. The inhibitory charge carried by fast and slow inhibition was equal in all experiments.

(B) Dynamic clamp studies were performed using excitatory conductances alone (black), and excitatory conductances accompanied by either fast inhibition (red), slow inhibition (blue), or mixed inhibition (purple). In all experiments, a small tonic inhibitory conductance (0.1–0.3 pS) was also present. Representative traces of granule cell spiking are shown for control (black), fast inhibition (red), slow inhibition (blue), and mixed inhibition (purple).

(C) Histograms of spike frequencies (normalized to the first 100 ms in control conditions) are plotted as a function of time for each condition (n = 17 cells).

relative to control conditions. Slow inhibition, on the other hand, dramatically suppressed spikes late in the train; the frequency decreased from 84% to 2% of control between the first and last bin. Thus, fast inhibition is more effective at suppressing spikes early in the train. In contrast, slow inhibition has very little influence on early spikes but dramatically suppresses spiking late in the train as the slow IPSC grows. Mixed inhibition had intermediate effects on granule cell firing (Figure 5C, purple). The initial firing rate was reduced by 45%, and the average spike rate during the last half of the train was 11% of the control firing rate (Figure 5C, purple), compared to 25% for fast inhibition (Figure 5C, red) and 3% for slow inhibition (Figure 5C, blue). This suggests that the fractional contribution of fast and slow inhibition will dictate how inhibition affects granule cell spike timing during ongoing mossy fiber activity.

The transfer function between excitatory synaptic input frequency and output spike rate determines the manner in which the information carried by those synapses is encoded. Inhibition may change the shape of the input-output curve by altering the slope or sensitivity to a given excitatory input, the range of input frequencies to which a given cell responds, or both. We used dynamic clamp to deliver regular trains of mossy fiber input across a range of frequencies between 10 Hz and 200 Hz to generate input-output curves for granule cells in response to these stimuli and tested the influence of fast, slow, and mixed trains of inhibition (as in Figure 5A). We focused on a simple case in which a single mossy fiber was active at regular frequencies and a single Golgi cell was active at one fixed frequency. Additional experimental information will be needed to extend

this approach to more complicated conditions that include irregular firing patterns, the activation of multiple mossy fibers and Golgi cells, coupling of Golgi cells through gap junctions (Dugue et al., 2009) and consideration of how the activity of mossy fibers and Golgi cells covaries under physiological conditions.

Raster plots of granule cell spiking in response to 40 Hz, 80 Hz, and 150 Hz trains of excitatory input in control conditions (Figure 6A, black), and with fast (Figure 6A, red), slow (Figure 6A, blue), or mixed (Figure 6A, purple) inhibition are shown. Fast inhibition and slow inhibition influenced the input-output curves in different ways. Over the course of the 1 s train the main influence of fast inhibition was a small rightward shift in the frequency range that activates granule cell spiking without a large change in slope (Figure 6B, red). Slow inhibition dramatically decreased the slope with minimal effect on the threshold (Figure 6B, blue). The effect of inhibition on the input-output curves evolved during the train due to the respective temporal dynamics of fast and slow inhibition. If spiking only in the first 100 ms is considered, the primary effect of inhibition was to decrease the slope, with fast inhibition being much more effective than slow inhibition (Figure 6C). Later in the train, when the dynamics of the synaptic conductances approach steady state, fast inhibition only modestly shifted the input-output curve while slow inhibition greatly reduced the gain of the input-output curve (Figure 6D). These findings indicate different roles for fast and slow inhibition in shaping the input-output curves at the mossy fiber → granule cell synapse. Mixed inhibition yielded input-output curves intermediate to those observed for fast inhibition and slow inhibition (Figures 6B–6D, purple). This suggests the
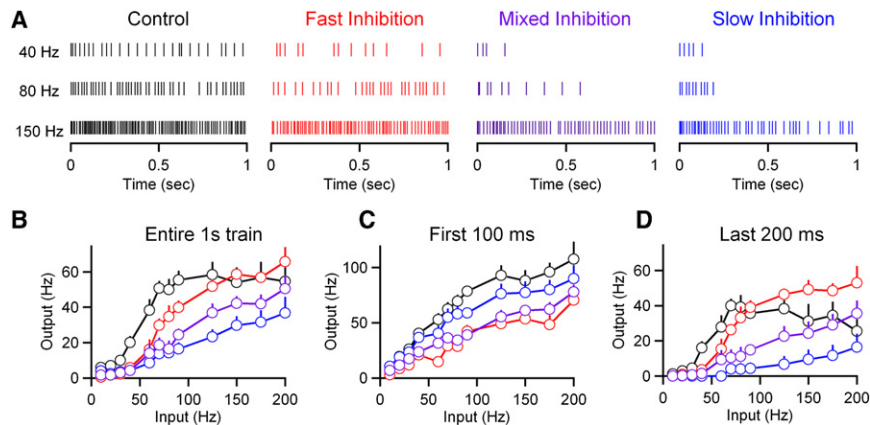
Figure 6. Fast and Slow Inhibition Differentially Alter the Input-Output Curve at the Mossy Fiber → Granule Cell Synapse

Dynamic clamp experiments were conducted as in Figure 5 with trains of mossy fiber activity at frequencies of 10 Hz to 200 Hz using excitatory conductances alone (black), and in the presence of fast inhibition (red), slow inhibition (blue), or mixed inhibition (purple).

(A) Raster plots of spikes evoked in granule cells at 40 Hz, 80 Hz, and 150 Hz are shown for each condition.

(B) Average input-output curves are shown with input frequencies corresponding to the frequency of mossy fiber input trains and output frequencies corresponding to granule cell spiking (n = 9 cells). Input-output curves from the same data set, considering only spiking in the first 100 ms (C) or last 200 ms (D) of the conductance injection.

proportion of fast and slow IPSC charge, which can vary between connections and across frequencies at a given connection, will determine the extent of shifts in threshold and slope.

DISCUSSION

Here we find that individual Golgi cell → granule cell connections exhibit IPSCs with diverse properties as a result of heterogeneity in the contribution of fast and slow IPSCs. The slow component of IPSCs becomes increasingly prominent during stimulus trains of 20 to 50 Hz. For granule cell spiking evoked by high-frequency mossy fiber trains, slow inhibition reduces spiking evoked late in the train, whereas fast inhibition is more effective early in the train. These two forms of inhibition differentially affect the input-output curve at the mossy fiber → granule cell synapse, with slow inhibition reducing the gain and fast inhibition increasing the threshold for evoking spikes.

The Frequency Dependence of Golgi Cell Inhibition

Previous studies have shown that inhibition evoked by extracellular stimulation at the Golgi cell → granule cell synapse has a fast component from direct synapses and a slow component from indirect spillover transmission (Rossi and Hamann, 1998). Here, we determined the properties of inhibition during trains of evoked activity and its dependence on stimulation frequency. At spontaneous Golgi cell firing rates (5–10 Hz; Holtzman et al., 2006; van Kan et al., 1993; Vos et al., 1999) fast and slow IPSCs make a roughly equivalent contribution to inhibitory charge transfer. As the frequency of extracellular stimulation increases the fast IPSC amplitude decreases, and the slow component grows to dominate charge transfer. Moreover the dynamics of the two components during a train differ markedly, as the fast IPSCs exhibit depression and the slow component gradually builds. Thus, the fast and slow components contribute in very different ways to the frequency dependence and dynamics of inhibition provided by Golgi cells.

Role of α_6-Containing GABA$_A$ Receptors

Granule cells express multiple GABA$_A$ receptor subtypes that may differentially contribute to fast and slow inhibition. High-

affinity, desensitization-resistant $\alpha_6\beta_{2/3}\delta$ receptors are preferentially extrasynaptic (Nusser et al., 1998). Deletion of the α_6 subunit or block of α_6-containing receptors eliminates a tonic GABA$_A$ conductance that is observed in granule cells (Brickley et al., 2001; Hamann et al., 2002; Rossi et al., 2003). However, blockade of α_6-containing receptors has variable effects on the amplitude and decay of single IPSCs (Hamann et al., 2002; Rossi and Hamann, 1998; Wall, 2002). In addition, both α_6- and α_1-containing receptors are detected at synapses and α_1-containing receptors can be found in extrasynaptic membranes (Nusser et al., 1995, 1998). We tested the possibility that during trains α_6-containing receptors preferentially mediate the slow component. The blockade of α_6-containing receptors did not alter the relative contribution of fast and slow components during trains (Figure S2), suggesting that α_6- and α_1-containing receptors both contribute to the fast and slow components.

Golgi Cell → Granule Cell Connections Are Heterogeneous

We observed diverse potencies (range: 10–78 pA, mean = 32 pA; n = 36), failure rates (range: 0–0.99, mean = 0.58; n = 36) and time courses ($A_{0.5}$ range: 1.5–58 ms, mean = 10.8; n = 42) in unitary IPSCs across Golgi cell → granule cell pairs. Differences in the number of direct synaptic contacts made by Golgi cells onto granule cells within a glomerulus have been observed (Jakab and Hamori, 1988), which could contribute to this diversity in synaptic properties. Moreover, granule cells typically have 1 to 4 dendrites (Palay and Chan-Palay, 1974), and it is possible that Golgi cells could contact glomeruli on multiple dendrites. Thus, a large variation in the number of direct synapses between different cell pairs may contribute to the wide range of potencies and failure rates we observe at individual connections. In addition, the distribution of Golgi cell synapses within a glomerulus may also be a factor in determining the balance of fast and slow IPSCs at a particular connection. The exclusively slow IPSCs (~12%, 5/42) we observe at some connections may reflect the observation that 40% of granule cells in a glomerulus are not directly contacted by a Golgi cell (Jakab and Hamori, 1988), if, as previously suggested (Rossi and Hamann, 1998), spillover generates slow IPSCs. Although it is also possible

that connections to some of the dendrites could have been lost during slicing, it is unlikely that this had a major influence on the properties of unitary IPSCs because care was taken to patch cells deep within the slice and granule cells have short dendrites.

Golgi cell diversity could also contribute to the diverse properties of the unitary IPSCs. While Golgi cells are glycinergic and GABAergic pacemaking interneurons with dendrites extending into molecular layer and a large profusely-ramifying axon (Dieudonne, 1998; Dugue et al., 2005; Forti et al., 2006; Kaneda et al., 1995; Ottersen et al., 1988; Palay and Chan-Palay, 1974), they differ in their soma size and in the expression of markers such as neurogranin and mGluR2 (Geurts et al., 2001; Neki et al., 1996; Simat et al., 2007). It will be of interest to determine if the synaptic diversity correlates with Golgi cell neurochemical phenotype.

Slow IPSCs Can Arise from Activity in a Single Golgi Cell

We demonstrate that realistic trains of activity in a single Golgi cell are sufficient to drive slow IPSCs at individual connections. These findings establish that the slow component of inhibition does not require the synchronous activation of multiple Golgi cells. Interestingly, isolated slow IPSCs are observed during trains in a small fraction of pairs, suggesting that lack of a direct morphological connection does not preclude a significant inhibitory drive from a Golgi cell.

Fast and Slow IPSCs Differentially Affect Synaptic Integration

Dynamic clamp experiments revealed that fast and slow IPSCs differentially influence spiking evoked by trains of mossy fiber activation. Slow inhibition strongly suppresses late spikes but has minimal influence on spiking early in a train. In contrast, fast inhibition is more effective at reducing granule cell spiking early in the train. In this way, sustained mossy fiber activation evokes a brief burst of granule cell spikes early in a train or more sustained spiking throughout the train depending on whether inhibition is dominated by slow or fast IPSCs, respectively.

These findings have important implications for models of cerebellar learning, such as eye-blink conditioning. A leading model of eye-blink conditioning requires that a continuous tone elevates spiking in different granule cells at different times following the onset of the tone (Medina et al., 2000). Only those synapses from granule cells that are active just prior to a puff of air to the eye will undergo plasticity, and in this way an animal can learn to close its eye immediately prior to an expected air puff. Our dynamic clamp experiments show that sustained mossy fiber activity, as might occur during a continuous tone (Aitkin and Boyd, 1978; Freeman and Muckler, 2003), can evoke firing in its granule cell targets with very different timing depending upon the relative contributions of fast and slow inhibition from Golgi cells. In this way, the two components of inhibition we describe could be crucial to timing-dependent cerebellar behaviors such as eye-blink conditioning.

Golgi cell inhibition alters the threshold and gain of the input-output curves relating mossy fiber activity to granule cell activity. This is critical for controlling the fraction of active granule cells during sensorimotor activity. Previous studies at this synapse demonstrate that tonic inhibition increases the threshold of the input-output curve and can reduce gain when converging inputs are noisy (Mitchell and Silver, 2003) or when synaptic depression causes the relationship between excitatory conductance and input frequency to become sublinear (Rothman et al., 2009). Here, we have found that fast and slow IPSCs evoked by trains of Golgi cell activity differentially influence the input-output curve of the granule cell in response to regular, depressing trains of mossy fiber input. Slow IPSCs preferentially reduce the gain whereas fast IPSCs preferentially increase the threshold. These findings suggest that the same Golgi cell can have very different effects on the input-output curves of the various granule cells it targets.

Fast and Slow Inhibition in Other Brain Regions

Slow forms of inhibition through ionotropic receptors are observed in several brain regions and may entail phasic events with very slow decay times (Bacci et al., 2003; Banks et al., 2000; Price et al., 2005; Sceniak and Maciver, 2008; Szabadics et al., 2007), long-lasting asynchronous release (Best and Regehr, 2009; Hefft and Jonas, 2005; Lu and Trussell, 2000), or tonic forms of inhibition that depend more on firing rate (Balakrishnan et al., 2009; Glykys and Mody, 2007a, 2007b; Park et al., 2007). In some brain regions, different interneuron subtypes are known to provide either fast or slow inhibition (Banks et al., 2000; Hefft and Jonas, 2005; Szabadics et al., 2007). Thus, distinct cell types may differentially control the input-output curves of principal cells in these regions. In contrast, because Golgi cells are the sole source of inhibition to cerebellar granule cells, the fractional contribution of fast and slow inhibition must be regulated to control the properties of the input-output curves and the timing-dependence of the target cell response.

EXPERIMENTAL PROCEDURES

Preparation of Brain Slices

Sagittal slices (250 μm thick) were prepared from the cerebellar vermis of 19- to 40-day-old Sprague-Dawley rats which were deeply anesthetized with halothane or isoflurane. Brains were dissected and sliced at 4°C in a cutting solution consisting of (in mM) 83 NaCl, 2.4 KCl, 0.5 CaCl₂, 6.8 MgCl₂, 24 NaHCO₃, 1.4 NaH₂PO₄, 24 glucose, and 71 sucrose. Slices were immediately transferred to cutting solution at 32°C and maintained for at least 30 min, then transferred to an external solution consisting of (in mM) 125 NaCl, 2.5 KCl, 2 CaCl₂, 1 MgCl₂, 26 NaHCO₃, 1.25 NaH₂PO₄, and 25 glucose. Slices were superfused at 2–3 ml/min with external solution bubbled with 95% O₂/5% CO₂.

Electrophysiology

Whole-cell voltage clamp recordings of granule cells and on-cell voltage clamp recordings of Golgi cells were obtained from visually identified cells in the granule cell layer using glass pipettes of 2–5 MΩ, when filled with a internal recording solution consisting of (in mM) 35 CsF, 100 CsCl, 10 EGTA, 10 HEPES (adjusted to pH 7.2 with CsOH). For whole-cell recordings, the access resistance and leak current were monitored, and experiments were rejected if either of these parameters changed significantly. GABAₐ-mediated synaptic currents were recorded at −60 mV in the presence of NBQX (10 μM) and R-CPP (5 μM) to block AMPAR-mediated synaptic currents and NMDAR-mediated synaptic currents, respectively. For experiments involving extracellular stimulation, a 1–2 MΩ glass pipette filled with external solution was used and trains were delivered every 60 s. Paired recordings were attempted for Golgi and granule cell pairs whose somas were typically separated by

approximately 300 μm or less. The internal solution for whole-cell current clamp and voltage clamp recordings of Golgi cells, and dynamic clamp recordings of granule cells consisted of (in mM) 130 KMeSO$_4$, 10 NaCl, 2 MgCl$_2$, 0.16 CaCl$_2$, 0.5 EGTA, 10 HEPES, 4 Na ATP, 0.4 Na GTP, 14 Tris-phosphocreatine (adjusted to pH 7.3 with KOH). Experiments were performed at 32°C–35°C. Outputs from an Axopatch 700A (Axon Instruments, Foster City, CA) amplifier were digitized with an ITC-18 A/D converter using custom routines (written by M.A. Xu-Friedman, State University of New York at Buffalo) in Igor Pro (Wavemetrics, Lake Oswego, OR). Recordings were sampled at 50 kHz and filtered for display at 1–5 kHz.

Data Analysis

The estimation of the slow IPSC during trains was performed by averaging the last 5 ms of the interval between two stimuli and setting the current amplitude within that interval equal to this average. This is shown in more detail in Figure S1. Synaptic events were detected using a threshold (average peak to peak noise in the baseline) of the first derivative, second derivative, and raw current trace, and confirmed visually. Data are expressed as mean ± SEM.

Preparation of Lentivirus

Lentivirus for the expression of channelrhodopsin-2 (ChR2) was prepared by transfection of HEK293 FT cells with (1) pLenti-synapsin I-hChR2-mCherry (K. Deisseroth, Stanford), (2) pCMV-Δ8.74, and (3) pCMV-VsVg. Virus was collected by ultracentrifugation, resuspended in PBS, and stored at −80°C. Lentivirus was delivered via stereotaxic injection into rats aged postnatal day (p) 12 to p15. Two holes were drilled in the skull 2–4 mm caudally from λ and ±2 mm from the midline, and virus was injected at a depth of approximately 1–3 mm below the surface of the brain. Injections (50 nl) were given every 20 s, and the total volume per injection site was between 1 and 2 μl. Acute slices were cut at least 6 days after virus injection. Cells expressing ChR2 were visually identified using mCherry fluorescence. Golgi and Purkinje cells were primarily labeled. Golgi cells were identified based on the size, shape, and location of their soma, as well as their spontaneous firing pattern. Typically fewer than 20 ChR2-expressing Golgi cells were observed in a slice, and their density decreased with distance from the injection site.

Photostimulation

ChR2-expressing cells were activated with a blue laser (Opto Engine 473 nm, 50 mW) with a Q495LP dichroic and a HQ: 525/50 emission filter (Chroma, Rockingham, VT). The size of the stimulation window was adjusted to closely box in the soma of the expressing Golgi cell (typically 20–30 μm in diameter, using an Olympus fluorescence attachment (modified by Till photonics) in order to minimize direct illumination of the Golgi cell axon. Short duration light pulses (typically 1 ms) were delivered and the intensity was adjusted to achieve reliable single spikes in response to single light pulses. Trains of varying frequency (5–100 Hz) were delivered every 60 s and the spiking of the Golgi cell was always monitored with an on-cell electrode containing Cs-based internal solution.

Dynamic Clamp

Dynamic clamp recordings were made using the built in dynamic clamp mode of the ITC-18 (Instrutech, Great Neck, NY). Conductance trains for the AMPAR and NMDAR components of mossy fiber EPSCs were constructed by convolving individual events using parameters obtained from voltage-clamp recordings of AMPA and NMDA mediated trains of synaptic events at the mossy fiber to granule cell synapse (Figure S3). AMPAR and NMDAR conductances reversed at 0 mV. NMDAR to AMPAR ratios were 0.1–0.5, in the range observed previously at this synapse (Cathala et al., 2000). A custom IGOR XOP (written by M.A. Xu-Friedman, State University of New York at Buffalo) interacting with a PCI-MIO-16XE-10 board (National Instruments, Austin, TX) was used for online generation of NMDA conductances. The voltage dependence of the NMDA component was approximated by the equation $I(t) = (V_{rev} - V_m) G_{NMDA}(t)/(1 + \exp(V_{1/2} - V_m)/V_{rate})$, where V_{rev} is the reversal potential (0 mV), V_m is the recorded membrane potential, $V_{1/2}$ is the membrane potential for half-maximal activation (−11 mV), and V_{rate} specifies the rate of dependence on membrane potential (18 mV). The reversal potential for inhibitory conductances was set at −75 mV (Mitchell and Silver, 2003; Rothman et al., 2009).

Dynamic clamp recordings were performed in the presence of NBQX (10 μM), CPP (5 μM), and picrotoxin (50 μM). Current was injected to maintain the membrane potential of the granule cell between −75 and −80 mV.

Reagents

All chemicals were from Sigma/RBI (St. Louis, MO) except CPP, CGP 55845, and NBQX (Tocris Cookson, Ellisville, MO).

SUPPLEMENTAL DATA

Supplemental Data include three figures and can be found with this article online at http://www.cell.com/neuron/supplemental/S0896-6273(09)00683-7.

REFERENCES

Aitkin, L.M., and Boyd, J. (1978). Acoustic input to the lateral pontine nuclei. Hear. Res. 1, 67–77.

Bacci, A., Rudolph, U., Huguenard, J.R., and Prince, D.A. (2003). Major differences in inhibitory synaptic transmission onto two neocortical interneuron subclasses. J. Neurosci. 23, 9664–9674.

Balakrishnan, V., Kuo, S.P., Roberts, P.D., and Trussell, L.O. (2009). Slow glycinergic transmission mediated by transmitter pooling. Nat. Neurosci. 12, 286–294.

Banks, M.I., White, J.A., and Pearce, R.A. (2000). Interactions between distinct GABA(A) circuits in hippocampus. Neuron 25, 449–457.

Best, A.R., and Regehr, W.G. (2009). Inhibitory regulation of electrically coupled neurons in the inferior olive is mediated by asynchronous release of GABA. Neuron 62, 555–565.

Boyden, E.S., Zhang, F., Bamberg, E., Nagel, G., and Deisseroth, K. (2005). Millisecond-timescale, genetically targeted optical control of neural activity. Nat. Neurosci. 8, 1263–1268.

Brickley, S.G., Cull-Candy, S.G., and Farrant, M. (1996). Development of a tonic form of synaptic inhibition in rat cerebellar granule cells resulting from persistent activation of GABAA receptors. J. Physiol. 497, 753–759.

Brickley, S.G., Revilla, V., Cull-Candy, S.G., Wisden, W., and Farrant, M. (2001). Adaptive regulation of neuronal excitability by a voltage-independent potassium conductance. Nature 409, 88–92.

Cathala, L., Misra, C., and Cull-Candy, S. (2000). Developmental profile of the changing properties of NMDA receptors at cerebellar mossy fiber-granule cell synapses. J. Neurosci. 20, 5899–5905.

Chance, F.S., Abbott, L.F., and Reyes, A.D. (2002). Gain modulation from background synaptic input. Neuron 35, 773–782.

Cobb, S.R., Buhl, E.H., Halasy, K., Paulsen, O., and Somogyi, P. (1995). Synchronization of neuronal activity in hippocampus by individual GABAergic interneurons. Nature 378, 75–78.

Dieudonne, S. (1998). Submillisecond kinetics and low efficacy of parallel fibre-Golgi cell synaptic currents in the rat cerebellum. J. Physiol. 510, 845–866.

DiGregorio, D.A., Nusser, Z., and Silver, R.A. (2002). Spillover of glutamate onto synaptic AMPA receptors enhances fast transmission at a cerebellar synapse. Neuron 35, 521–533.

Dugue, G.P., Dumoulin, A., Triller, A., and Dieudonne, S. (2005). Target-dependent use of co-released inhibitory transmitters at central synapses. J. Neurosci. 25, 6490–6498.

Dugue, G.P., Brunel, N., Hakim, V., Schwartz, E., Chat, M., Levesque, M., Courtemanche, R., Lena, C., and Dieudonne, S. (2009). Electrical coupling mediates tunable low-frequency oscillations and resonance in the cerebellar Golgi cell network. Neuron 61, 126–139.

Eccles, J., Ito, M., and Szentagothai, J. (1967). The Cerebellum as a Neuronal Machine (New York: Springer-Verlag).

Farrant, M., and Brickley, S.G. (2003). Properties of GABAA receptor-mediated transmission at newly formed Golgi-granule cell synapses in the cerebellum. Neuropharmacology 44, 181–189.

Forti, L., Cesana, E., Mapelli, J., and D'Angelo, E. (2006). Ionic mechanisms of autorhythmic firing in rat cerebellar Golgi cells. J. Physiol. 574, 711–729.

Freeman, J.H., Jr., and Muckler, A.S. (2003). Developmental changes in eyeblink conditioning and neuronal activity in the pontine nuclei. Learn. Mem. 10, 337–345.

Freund, T.F., and Buzsaki, G. (1996). Interneurons of the hippocampus. Hippocampus 6, 347–470.

Geurts, F.J., Timmermans, J., Shigemoto, R., and De Schutter, E. (2001). Morphological and neurochemical differentiation of large granular layer interneurons in the adult rat cerebellum. Neuroscience 104, 499–512.

Glickfeld, L.L., and Scanziani, M. (2006). Distinct timing in the activity of cannabinoid-sensitive and cannabinoid-insensitive basket cells. Nat. Neurosci. 9, 807–815.

Glykys, J., and Mody, I. (2007a). Activation of GABAA receptors: views from outside the synaptic cleft. Neuron 56, 763–770.

Glykys, J., and Mody, I. (2007b). The main source of ambient GABA responsible for tonic inhibition in the mouse hippocampus. J. Physiol. 582, 1163–1178.

Gupta, A., Wang, Y., and Markram, H. (2000). Organizing principles for a diversity of GABAergic interneurons and synapses in the neocortex. Science 287, 273–278.

Hamann, M., Rossi, D.J., and Attwell, D. (2002). Tonic and spillover inhibition of granule cells control information flow through cerebellar cortex. Neuron 33, 625–633.

Hamori, J., and Somogyi, J. (1983). Differentiation of cerebellar mossy fiber synapses in the rat: a quantitative electron microscope study. J. Comp. Neurol. 220, 365–377.

Hefft, S., and Jonas, P. (2005). Asynchronous GABA release generates long-lasting inhibition at a hippocampal interneuron-principal neuron synapse. Nat. Neurosci. 8, 1319–1328.

Holtzman, T., Mostofi, A., Phuah, C.L., and Edgley, S.A. (2006). Cerebellar Golgi cells in the rat receive multimodal convergent peripheral inputs via the lateral funiculus of the spinal cord. J. Physiol. 577, 69–80.

Jakab, R.L., and Hamori, J. (1988). Quantitative morphology and synaptology of cerebellar glomeruli in the rat. Anat. Embryol. (Berl.) 179, 81–88.

Kaneda, M., Farrant, M., and Cull-Candy, S.G. (1995). Whole-cell and single-channel currents activated by GABA and glycine in granule cells of the rat cerebellum. J. Physiol. 485, 419–435.

Klausberger, T., Magill, P.J., Marton, L.F., Roberts, J.D., Cobden, P.M., Buzsaki, G., and Somogyi, P. (2003). Brain-state- and cell-type-specific firing of hippocampal interneurons in vivo. Nature 421, 844–848.

Korpi, E.R., Kuner, T., Seeburg, P.H., and Luddens, H. (1995). Selective antagonist for the cerebellar granule cell-specific gamma-aminobutyric acid type A receptor. Mol. Pharmacol. 47, 283–289.

Lu, T., and Trussell, L.O. (2000). Inhibitory transmission mediated by asynchronous transmitter release. Neuron 26, 683–694.

Markram, H., Toledo-Rodriguez, M., Wang, Y., Gupta, A., Silberberg, G., and Wu, C. (2004). Interneurons of the neocortical inhibitory system. Nat. Rev. Neurosci. 5, 793–807.

McBain, C.J., and Fisahn, A. (2001). Interneurons unbound. Nat. Rev. Neurosci. 2, 11–23.

Medina, J.F., Nores, W.L., Ohyama, T., and Mauk, M.D. (2000). Mechanisms of cerebellar learning suggested by eyelid conditioning. Curr. Opin. Neurobiol. 10, 717–724.

Miles, R., Toth, K., Gulyas, A.I., Hajos, N., and Freund, T.F. (1996). Differences between somatic and dendritic inhibition in the hippocampus. Neuron 16, 815–823.

Mitchell, S.J., and Silver, R.A. (2000a). GABA spillover from single inhibitory axons suppresses low-frequency excitatory transmission at the cerebellar glomerulus. J. Neurosci. 20, 8651–8658.

Mitchell, S.J., and Silver, R.A. (2000b). Glutamate spillover suppresses inhibition by activating presynaptic mGluRs. Nature 404, 498–502.

Mitchell, S.J., and Silver, R.A. (2003). Shunting inhibition modulates neuronal gain during synaptic excitation. Neuron 38, 433–445.

Neki, A., Ohishi, H., Kaneko, T., Shigemoto, R., Nakanishi, S., and Mizuno, N. (1996). Metabotropic glutamate receptors mGluR2 and mGluR5 are expressed in two non-overlapping populations of Golgi cells in the rat cerebellum. Neuroscience 75, 815–826.

Nielsen, T.A., DiGregorio, D.A., and Silver, R.A. (2004). Modulation of glutamate mobility reveals the mechanism underlying slow-rising AMPAR EPSCs and the diffusion coefficient in the synaptic cleft. Neuron 42, 757–771.

Nusser, Z., Roberts, J.D., Baude, A., Richards, J.G., and Somogyi, P. (1995). Relative densities of synaptic and extrasynaptic GABAA receptors on cerebellar granule cells as determined by a quantitative immunogold method. J. Neurosci. 15, 2948–2960.

Nusser, Z., Sieghart, W., and Somogyi, P. (1998). Segregation of different GABAA receptors to synaptic and extrasynaptic membranes of cerebellar granule cells. J. Neurosci. 18, 1693–1703.

Ottersen, O.P., Storm-Mathisen, J., and Somogyi, P. (1988). Colocalization of glycine-like and GABA-like immunoreactivities in Golgi cell terminals in the rat cerebellum: a postembedding light and electron microscopic study. Brain Res. 450, 342–353.

Palay, S., and Chan-Palay, V. (1974). Cerebellar Cortex Cytology and Organization (New York: Springer-Verlag).

Park, J.B., Skalska, S., Son, S., and Stern, J.E. (2007). Dual GABAA receptor-mediated inhibition in rat presympathetic paraventricular nucleus neurons. J. Physiol. 582, 539–551.

Payne, J.A. (1997). Functional characterization of the neuronal-specific K-Cl cotransporter: implications for [K+]o regulation. Am. J. Physiol. 273, C1516–C1525.

Pouille, F., and Scanziani, M. (2001). Enforcement of temporal fidelity in pyramidal cells by somatic feed-forward inhibition. Science 293, 1159–1163.

Pouille, F., and Scanziani, M. (2004). Routing of spike series by dynamic circuits in the hippocampus. Nature 429, 717–723.

Price, C.J., Cauli, B., Kovacs, E.R., Kulik, A., Lambolez, B., Shigemoto, R., and Capogna, M. (2005). Neurogliaform neurons form a novel inhibitory network in the hippocampal CA1 area. J. Neurosci. 25, 6775–6786.

Rossi, D.J., and Hamann, M. (1998). Spillover-mediated transmission at inhibitory synapses promoted by high affinity alpha6 subunit GABA(A) receptors and glomerular geometry. Neuron 20, 783–795.

Rossi, D.J., Hamann, M., and Attwell, D. (2003). Multiple modes of GABAergic inhibition of rat cerebellar granule cells. J. Physiol. 548, 97–110.

Rothman, J.S., Cathala, L., Steuber, V., and Silver, R.A. (2009). Synaptic depression enables neuronal gain control. Nature 457, 1015–1018.

Sceniak, M.P., and Maciver, M.B. (2008). Slow GABA(A) mediated synaptic transmission in rat visual cortex. BMC Neurosci. 9, 8.

Silver, R.A., Cull-Candy, S.G., and Takahashi, T. (1996). Non-NMDA glutamate receptor occupancy and open probability at a rat cerebellar synapse with single and multiple release sites. J. Physiol. 494, 231–250.

Simat, M., Parpan, F., and Fritschy, J.M. (2007). Heterogeneity of glycinergic and gabaergic interneurons in the granule cell layer of mouse cerebellum. J. Comp. Neurol. *500*, 71–83.

Somogyi, P., and Klausberger, T. (2005). Defined types of cortical interneurone structure space and spike timing in the hippocampus. J. Physiol. *562*, 9–26.

Szabadics, J., Tamas, G., and Soltesz, I. (2007). Different transmitter transients underlie presynaptic cell type specificity of GABAA,slow and GABAA,fast. Proc. Natl. Acad. Sci. USA *104*, 14831–14836.

Tamas, G., Lorincz, A., Simon, A., and Szabadics, J. (2003). Identified sources and targets of slow inhibition in the neocortex. Science *299*, 1902–1905.

van Kan, P.L., Gibson, A.R., and Houk, J.C. (1993). Movement-related inputs to intermediate cerebellum of the monkey. J. Neurophysiol. *69*, 74–94.

Vogels, T.P., and Abbott, L.F. (2009). Gating multiple signals through detailed balance of excitation and inhibition in spiking networks. Nat. Neurosci. *12*, 483–491.

Vos, B.P., Volny-Luraghi, A., and De Schutter, E. (1999). Cerebellar Golgi cells in the rat: receptive fields and timing of responses to facial stimulation. Eur. J. Neurosci. *11*, 2621–2634.

Wall, M.J. (2002). Furosemide reveals heterogeneous GABA(A) receptor expression at adult rat Golgi cell to granule cell synapses. Neuropharmacology *43*, 737–749.

Wall, M.J., and Usowicz, M.M. (1997). Development of action potential-dependent and independent spontaneous GABAA receptor-mediated currents in granule cells of postnatal rat cerebellum. Eur. J. Neurosci. *9*, 533–548.

Watanabe, D., Inokawa, H., Hashimoto, K., Suzuki, N., Kano, M., Shigemoto, R., Hirano, T., Toyama, K., Kaneko, S., Yokoi, M., et al. (1998). Ablation of cerebellar Golgi cells disrupts synaptic integration involving GABA inhibition and NMDA receptor activation in motor coordination. Cell *95*, 17–27.

Wehr, M., and Zador, A.M. (2003). Balanced inhibition underlies tuning and sharpens spike timing in auditory cortex. Nature *426*, 442–446.

Xu-Friedman, M.A., and Regehr, W.G. (2003). Ultrastructural contributions to desensitization at cerebellar mossy fiber to granule cell synapses. J. Neurosci. *23*, 2182–2192.